

BENEFITS OF INCLUSION OF GEOSYNTHETIC PRODUCTS IN REINFORCEMENT
OF FLEXIBLE AIRFIELD PAVEMENTS USING THREE-DIMENSIONAL FINITE
ELEMENT MODELING

By:

Cesar Tirado, Cesar Carrasco, and Soheil Nazarian
Center for Transportation Infrastructure Systems (CTIS)
The University of Texas at El Paso
500 W. University Ave., Metallurgy Bldg. M-104
El Paso, TX, 79968-0516
USA

Phone: (915) 747-6925; Fax: (915) 747-8037

ctirado@utep.edu

ccarras@utep.edu

nazarian@utep.edu

and

Gregory J. Norwood and Jeb S. Tingle
United States Army Corps of Engineers
Engineer Research and Development Center (ERDC)
3909 Halls Ferry Rd.
Vicksburg, MS 39180-6199
USA

Phone: (601) 634-3111

Gregory.J.Norwood@usace.army.mil

Jeb.S.Tingle@usace.army.mil

PRESENTED FOR THE
2014 FAA WORLDWIDE AIRPORT TECHNOLOGY TRANSFER CONFERENCE
Galloway, New Jersey, USA

August 2014

ABSTRACT

A 3D finite element model was developed to estimate the structural benefits that are gained by introducing the geosynthetic materials within pavements. Modeling of the geosynthetic material was carried out by means of membrane and interface elements. The most relevant properties, including the type of geosynthetic used (geomembrane or geogrid), soil-geogrid interface shear stiffness, and the type of geogrid (biaxial vs. triaxial), were evaluated. In addition, the impacts of pavement structural properties, linear vs. nonlinear material models, and location of reinforcement were evaluated. The benefits provided by the geosynthetic reinforcement depended on the pavement structure and the airplane wheel configuration and pressure.

INTRODUCTION

Construction of flexible airfield pavements requires the use of high-quality aggregates; yet, in regions where these materials are in short supply, marginal materials must be used instead. A number of geosynthetic products are marketed for the reinforcement of base materials. These products can be used to increase the stiffness of the marginal base course materials, thereby reducing the required thickness of the marginal bases. Three main categories of geosynthetics are used to reinforce unbound layers: geogrids, geotextiles and geocomposites. Geotextiles exhibit some tensile strength and can be used to complement soils that carry compressional loads but weak in tension. Geotextile reinforcement can be more beneficial on low strength fine-grained silts or clayey soils. Geogrids are currently being used by many transportation agencies to reinforce soils in many applications, including embankments, levees, steep slopes, retaining walls, and roadways. It is believed that the most benefit occurs when there is good interlock between the granular material and the grid as larger aggregate particles partly stick out through the grid apertures. Geogrids prevent aggregate material from moving laterally under applied loads and enhances local strengthening and stiffness in the base layer. The higher stiffness zone around the geogrid essentially benefits pavement response by better bridging over the weak subgrade soil and transmitting reduced critical stresses and strains on top of subgrade.

Several organizations in the past 20 years have studied the benefits provided by of geosynthetics placed within the unbound aggregate layers in flexible pavement systems [1]. Generally, structural benefits of including geosynthetic reinforcement are dependent on pavement design parameters such as thickness of the pavement section, strength and/or stiffness of the subgrade, and properties and type of geosynthetic used [1]. The primary benefits suggested are the extension of service life or a reduction in the thickness of the pavement structure. Traffic Benefit Ratio (TBR) and Base Course Reduction Ratio (BCR) have been typically used to evaluate the benefits and to estimate the increase in service life of a pavement [2].

FINITE ELEMENT MODEL

To quantify the benefits of the geosynthetic reinforced pavements a 3-D finite element model that simulates flexible pavement sections with and without geosynthetic reinforcement was developed. The finite element model consisted of an isotropic linear elastic model based on the generalized Hooke's Law. However, to account for the nonlinear behavior of the pavement structural layers, a nonlinear material model was also incorporated into the FE model. The

following material model proposed by Uzan [3], which is applicable to fine and coarse grained base and subgrade materials, was used.

$$E = k_1 \sigma_c^{k_2} \sigma_d^{k_3} \quad (1)$$

where E is the modulus, σ_c and σ_d are the confining pressure and the deviatoric stress, respectively; parameters k_1 , k_2 , and k_3 are coefficients statistically determined from the results of laboratory resilient modulus tests.

A three-noded triangular membrane element was formulated to model the geomembrane reinforcement. The membrane element was modeled based a plane stress formulation. This element was incorporated into the model by taking advantage of the triangular faces of the tetrahedral elements lying along the plane corresponding to the location of the geomembrane. In order to model the geogrid, interface elements were included. The geogrid and soil-geogrid interaction were modeled via the inclusion of membrane and interface elements, respectively. The plane stress geogrid membrane element consisted of three nodes and the interface element had a linear elastic relation. This relation is given by

$$\begin{Bmatrix} d\sigma_n \\ d\tau_x \\ d\tau_z \end{Bmatrix} = \begin{bmatrix} k_n & 0 & 0 \\ 0 & k_s & 0 \\ 0 & 0 & k_s \end{bmatrix} \begin{Bmatrix} dv \\ du \\ dw \end{Bmatrix}, \quad (2)$$

where the constitutive model shows the two stiffness values of k_n and k_s that stand for normal stiffness and shear stiffness, respectively. The three displacement components are v , u , and w . The normal stress is represented with σ_n and τ represents shear stresses acting in different directions. Figure 1 shows the model, as well as the reinforcement location relative to the pavement system. The layers above and below the reinforcement were modeled with tetrahedral elements containing four nodes, while the interface elements contained 6 nodes.

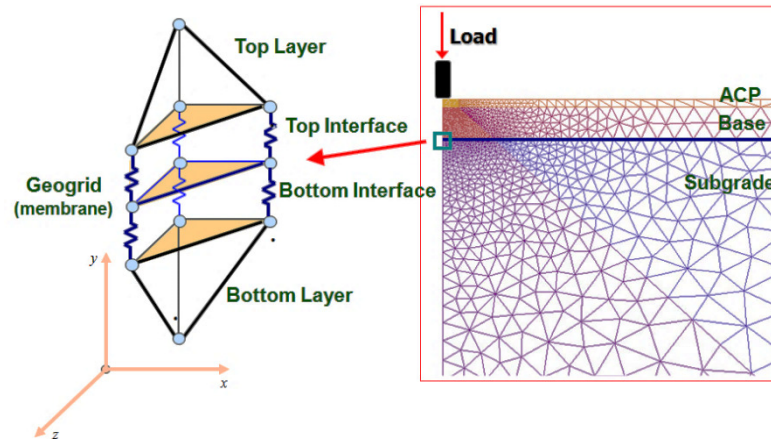


Figure 1. Illustration of Modeled Pavement System and Reinforcement.

DISTRESS MODELS

Two failure mechanisms were taken into consideration: permanent deformation (rutting) and fatigue cracking. To predict rutting a constitutive model was used for all pavement layers in the form of

$$\varepsilon_p = \frac{\mu}{1-\alpha} \cdot \varepsilon_r \cdot N^{1-\alpha}, \quad (3)$$

where ε_p is the accumulated permanent strain, ε_r is the resilient elastic strain, N is the load cycle number and α and μ are material parameters measured in the laboratory: the rate of increase in permanent deformation against the number of load applications and the permanent deformation, respectively. The total elastic strain within a pavement layer is simply the total compression of that layer [4].

Alligator fatigue cracking is assumed to be generated from tensile strains ε_t occurring at the bottom of the asphalt layers (bottom-up cracking). The Asphalt Institute MS-1 model used to predict fatigue is given by

$$N_f = k_1 \varepsilon_t^{-k_2} E_{ACP}^{-k_3}, \quad (4)$$

where N_f is the number of load applications to failure, ε_t is the tensile strain at the bottom of the asphalt layer, E_{ACP} is the asphalt modulus, $k_1 = 0.0796$, $k_2 = 3.291$, and $k_3 = 0.854$ are regression parameters based on a 50% wheel path failure area criterion [5].

PARAMETRIC STUDY

A series of sensitivity analyses was carried to assess the impact of a geosynthetic layer on the improvement of the life of a pavement. Some of the design parameters such as the layer thicknesses and the location of the geosynthetic layer were varied to study their impact on the pavement performance. Failure criteria were established to be 1 in. in rutting and 50% of area subjected to fatigue cracking.

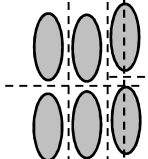
A three layer flexible pavement system, as shown in Figure 2 was considered in this study as the control pavement section. The control case did not include the geosynthetic layer. Unless indicated otherwise, the control case consisted of a 3 in. thick hot mix asphalt (HMA) layer with a modulus of 500 ksi, placed on top of a 10 in. base layer with modulus of 30 ksi, and subgrade with a modulus of 5 ksi to account for a CBR of 3.5. Other relevant properties are shown in the figure.

HMA	E = 500 ksi, H = 3 in., $\nu = 0.33$, $\alpha = 0.78$, $\mu = 0.25$
Base	E = 30 ksi, H = 10 in., $\nu = 0.33$, $\alpha = 0.75$, $\mu = 0.40$
Subgrade	E = 5 ksi, $\nu = 0.33$, $\alpha = 0.90$, $\mu = 0.40$

Figure 2. Control Pavement Section.

Two airplanes were considered for the parametric analysis: a C-17 Globemaster III cargo aircraft and an F-15E Eagle fighter plane. Properties of the landing gears for these aircrafts are summarized in Table 1. The C-17's landing gear system consists of a single nose strut with two wheels and two twin-strut tandem gears, one landing gear per side with three wheels per strut, i.e. a six-wheel gear, also called triple tandem tricycle (TRT or T-TA) landing gear. The F-15 has a retractable tricycle landing gear with single wheels for each landing gear.

Table 1.
Details of Aircraft Gears Considered for Parametric Studies.

Parameter	Aircraft type	
	C-17	F-15E Eagle
Maximum takeoff weight	585,000 lb (2600 kN)	81,000 lb (360 kN)
Landing gear designation and configuration	TRT - triple tandem tricycle	S – Single wheel
		
Landing gear load	269,217 lb (1200 kN)	70,470 lb (313.5 kN)
Strut spacing	93 in. (2.36 m)	-
Tire spacing	42 in. (1.07 m)	-
Dimensions	22.8 in. × 13.8 in. (580 mm × 350.5 mm)	13.4 in. × 8.1 in. (340 mm × 206 mm)
Contact area	314 in ² (202,580 mm ²)	108.5 in ² (69,700 mm ²)
Tire pressure	140 psi (965 kPa)	325 psi (2240 kPa)

Two types of geogrids were considered in this study: a biaxial, polypropylene geogrid, and a triaxial geogrid. The properties assumed for these materials are summarized in Table 2. Geogrids exhibit directional properties, e.g. the elastic modulus differs between the machine and cross-machine directions of the materials. The directions of the ribs are referred to as machine direction (MD), orientated in the direction of the manufacturing process or cross machine direction (XMD) perpendicular to the machine direction ribs [6].

Table 2.
Properties of Geogrids Assumed for Parametric Studies.

Type	Parameter	Properties	
		Machine Direction (MD)	Cross Machine Direction (XMD)
Biaxial	Minimum rib thickness	1.27 mm (0.05 in.)	1.27 mm (0.05 in.)
	Tensile strength @2% strain	6.0 kN/m (410 lb/ft)	9.0 kN/m (620 lb/ft)
	Aperture stability	650 N-mm/deg (5.7 lb-in./deg)	
Triaxial	Mid-rid depth	1.2 mm (0.05 in.)	1.2 mm (0.05 in.)
	Mid-rid width	1.1 mm (0.04 in.)	1.1 mm (0.04 in.)
	Tensile strength @0.5% strain	1.1 kN/m (77 lb/ft)	
	Aperture stability	300 N-mm/deg (2.6 lb-in./deg)	

The geogrid was placed in two locations for all studies: middle of the base layer and interface of the subgrade and base layer. To incorporate these properties into the FE model, they were transformed to linear elastic properties. The elastic modulus of the geogrid, E_g , is determined from the tensile stiffness, J_g , and the geogrid thickness, t , using

$$E_g = \frac{J_g}{t}, \quad (5)$$

where J_g can be estimated from the tensile strength, T_{ca} , at a certain level of axial strain, ε_a , from

$$J_g = \frac{T_{\varepsilon_a}}{\varepsilon_a}. \quad (6)$$

The geogrid shear modulus of geosynthetic materials is a parameter for which tests have not been specifically developed. However, a test apparatus and testing procedures were proposed by Kinney and Xiaolin [7] to determine a parameter called the aperture stability modulus. The geogrid shear modulus, G , is related to the measured aperture stability modulus, ASM, of the geosynthetics by

$$G = 7 \text{ ASM}, \quad (7)$$

where the shear modulus has units of kPa and the aperture stability modulus has units of N-mm/degree [8]. This formulation is valid for a reinforcement sheet assumed to have isotropic linear elastic properties. The ASM for each geosynthetic material is provided in Table 2. Tensile properties for the considered geosynthetics are summarized in Table 3.

Table 3.
Geosynthetic Tensile Properties.

Parameter	Geosynthetic	
	Biaxial	Triaxial
Modulus in machine direction, E_m	34 ksi (236 MPa)	26 ksi (177 MPa)
Modulus in cross machine direction, E_{xm}	52 ksi (356 MPa)	26 ksi (177 MPa)
Poisson's ratio in cross-machine – machine direction, ν_{xm-m}	0.25	0.25
Geogrid shear modulus in cross-machine – machine plane, G_{xm-m}	660 psi (4550 kPa)	305 psi (2100 kPa)

Besides the geosynthetic tensile properties used for the membrane elements, the interaction between the soil and the geogrid requires the inclusion of interface elements. Using the constitutive model shown in Equation 2, the normal and shear stiffnesses are required. Normal interface springs stiffness k_n was assigned a value of 9,000 kci (2,443 GPa/m) to maintain continuity and prevent overlapping and/or punching through the neighboring elements. The mechanism of soil and aggregate geogrid interaction has not been clearly identified and no standard testing technique is available to evaluate the soil-geogrid interface shear stiffness k_s . For modeling purposes other studies have used a soil-geogrid interface shear stiffness of 15 kci (4.1 GPa/m) for the biaxial geogrid [9].

The traffic benefit ratio (TBR) was used to assess the effectiveness of a geosynthetic material. TBR is defined as the ratio of the number of cycles to reach a certain rut depth for the reinforced pavement to that of the unreinforced pavement, which can be simply expressed as

$$TBR = \frac{N_{\text{geogrid reinforced}}}{N_{\text{unreinforced}}} \quad (8)$$

where N is the number of load repetitions to failure. This parameter has been commonly used to evaluate the effectiveness of geosynthetics in enhancing the service life. In this study, the TBR values were determined based on the rut depth of 1 in. (25 mm) since failure in rutting occurs

long before failure was reached in fatigue cracking for any of the pavements analyzed in this study.

GEOMEMBRANES VS. GEOGRIDS

The effectiveness of different geosynthetic materials was evaluated. The main difference between a geogrid material and a geomembrane/geotextile lies in the aperture size of the geosynthetics. Geogrids provide interlocking with base course aggregates due to their large aperture size and the stability of junctions whereas geotextiles lack this feature. Geotextiles are suitable to provide separation between the base and subgrade materials by preventing the mixing of subgrade soil and granular base materials. Consequently, geogrids provide greater shear stiffness compared to the geotextiles. Geotextiles are modeled by using a shear stiffness close to zero [10]. Properties of the geotextile used in the parametric study are shown in Table 4. Figure 3 presents a comparison of traffic benefit ratio for a geotextile and a biaxial geogrid placed at the base-subgrade interface for the control pavement section. Geomembrane/geotextile has minimal benefit for F-15 landing gears and detrimental impact under C-17 landing gears. The geogrid was more beneficial than geomembrane in terms of improving the life of the pavement.

Table 4. Properties of Geomembranes Assumed for Parametric Studies.

Type	Parameter	Properties	
		Machine Direction (MD)	Cross Machine Direction (XMD)
Geotextile: Amoco 2006	Tensile strength @2% strain	4.25 kN/m (290 lb/ft)	13.6 kN/m (930 lb/ft)
	Aperture stability		None

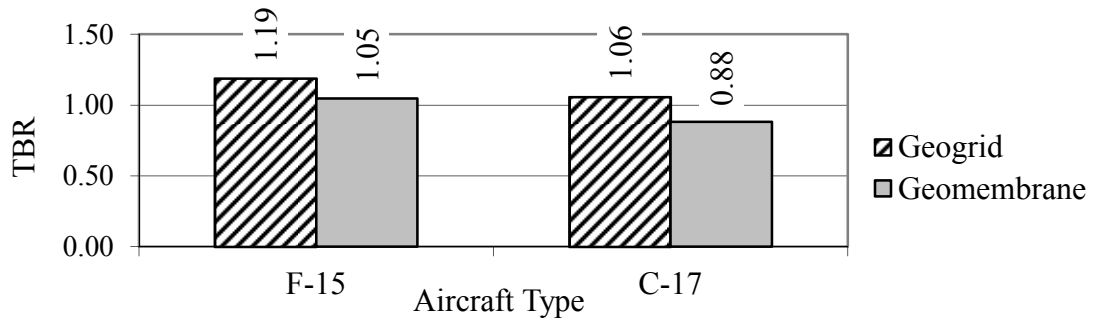


Figure 3. Traffic Benefit Ratio (TBR) for 3-in. HMA and 10 in. Base Geogrid and Geomembrane/Geotextile Pavements.

SOIL-GEOGRID INTERFACE SHEAR STIFFNESS, k_s

The effect of the soil-geogrid interface shear stiffness was studied for biaxial geogrid reinforced pavements. The shear stiffness was varied from 5,000 pci (1,400 MPa/m) to 500,000 pci (136 GPa/m). The variations in the number of F-15 passes to failure for the control section (3-in. HMA, 10-in. base as shown in Figure 2) with the soil-geogrid interface stiffness were estimated. The number of passes to failure increased slightly as the soil-geogrid interface shear stiffness increased. The traffic benefit ratios (TBRs), as shown in Figure 4, were almost independent of this parameter when the geogrid was placed at the base-subgrade interface. On the other hand, the TBR is sensitive to this parameter when the geogrid is placed at the mid-

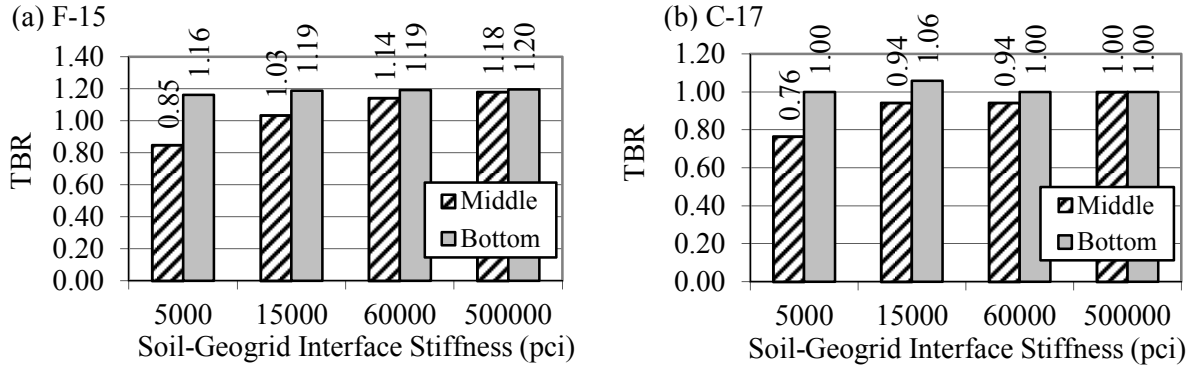


Figure 4. Variation of Traffic Benefit Ratio (TBR) with Respect to Soil-Geogrid Interface Stiffness in Rutting for a 3-in. Asphalt and 10 in. Base Pavement.

depth of the base. The same trends were observed for the C-17 landing gear; however, unlike the F-15, the TBRs indicated geogrids were either detrimental or not effective in mitigating rutting for the C-17 landing gear due to the much larger stresses experienced by the subgrade under the C-17 landing gear.

LINEAR ELASTIC VS. NONLINEAR MODELS FOR BASE AND SUBGRADE

To quantify the significance of utilizing a nonlinear constitutive model for the base and subgrade, a parametric study was carried out assuming the nonlinear parameters reflected in Table 5 for the generalized Uzan’s model. The nonlinear constants k_1 for both layers were set equal to the linear elastic modulus. The assigned parameters for the subgrade were set to simulate a clayey subgrade.

Table 5. Nonlinear Parameters for Base and Subgrade.

Layer	Nonlinear Parameters		
	k_1	k_2	k_3
Base	30,000 psi (207 MPa)	0.25	-0.25
Subgrade	5,000 psi (36 MPa)	0	-0.5

The TBR values from the nonlinear analyses, shown in Figure 5, decreased in comparison to those obtained from the linear elastic analysis for the F-15 landing gear for a range of base thicknesses varying from 8 to 18 in. Similar patterns were observed for the C-17 landing gear. However, the differences between the TBR values from the two analyses are smaller.

BIAXIAL VS. TRIAXIAL GEOGRIDS

Figure 6 shows the traffic benefit ratios for the biaxial and triaxial geogrids for a 3 in. asphalt pavement with varying base thicknesses for both aircrafts. The number of passes to failure increased for both biaxial and triaxial geogrids as the base thickness increased; however, the number of passes for the triaxial geogrid reinforcement did not prove to be as beneficial as the biaxial material, for both aircraft types. The triaxial geogrid had no effect when used at the bottom of the base layer, and was detrimental when used at the middle. This behavior may be

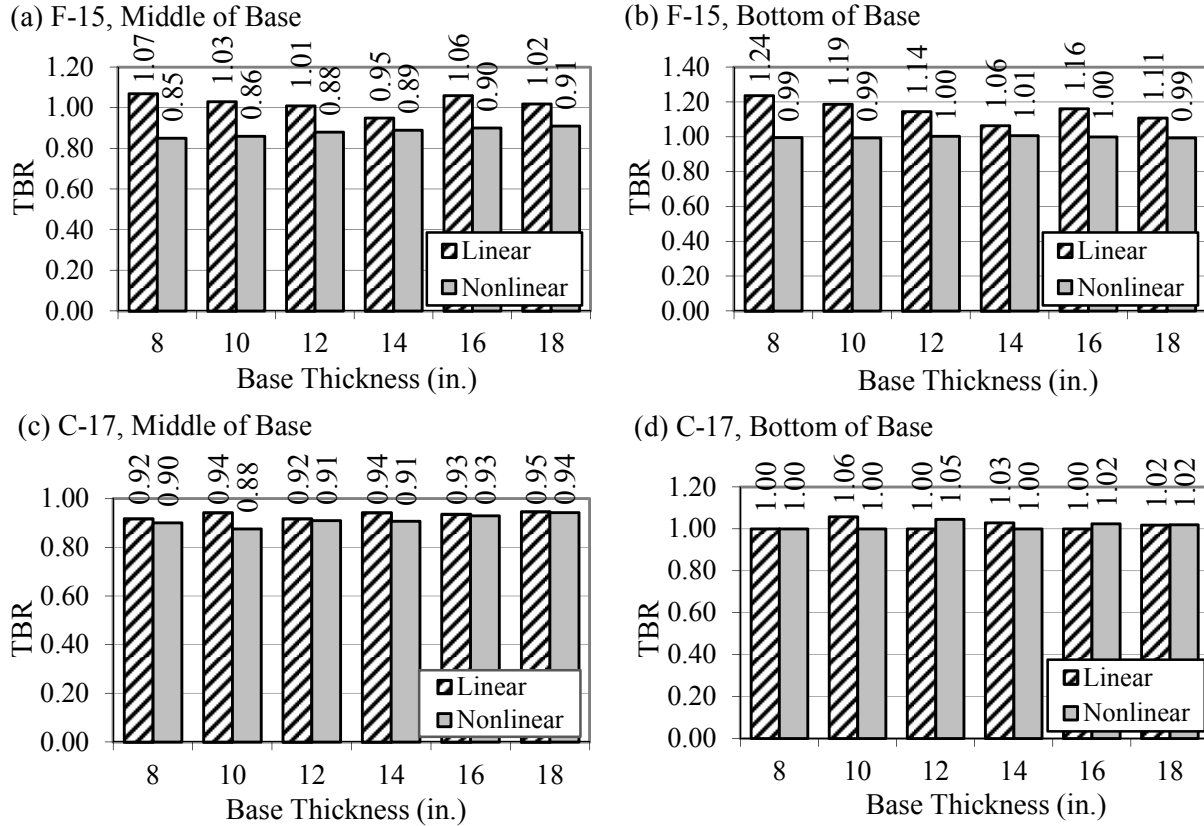


Figure 5. Variation of Traffic Benefit Ratio (TBR) with Respect to Base Thickness Using Linear Elastic and Nonlinear Models for a 3-in. Asphalt Pavement for F-15 and C-17 Aircrafts.

explained from the weaker properties of the triaxial geogrid assumed as compared to the biaxial geogrid.

IMPACT OF BASE AND HMA THICKNESS

Figure 7 presents the results for pavements with a geogrid placed at the middle of the base layer and at the bottom of the base layer (i.e. the subgrade-base interface) for both F-15 and C-17 aircrafts. The figure further includes the results for an unreinforced pavement with the same structure. As expected, the number of passes to failure increases as the base thickness increases, and the use of geogrid reinforcement extended the life of a pavement for both cases, especially when placed at the bottom of the base layer. Figure 8 shows the contribution of each layer to a rut depth of 1 in. for the same pavement and traffic. Layer contribution is marked with different shading. Columns with black background represent the rut depth for unreinforced pavements, while white and grey columns show the rut depth for pavements with geogrid reinforcement at the middle and at the bottom of the base layer, respectively. In the case of a pavement subjected to F-15 trafficking, as the base gets thicker, the base contributes from 18% to 42% of rutting, while the subgrade contributes a range of 81% to 57% of rutting. The asphalt layer did not contribute more than 0.5% of the total rutting. The proportion of rutting per layer remains the same when the geogrid is placed at the bottom of the base when compared to an unreinforced pavement. However, when reinforcement is placed at the middle of the base, the stresses transfer

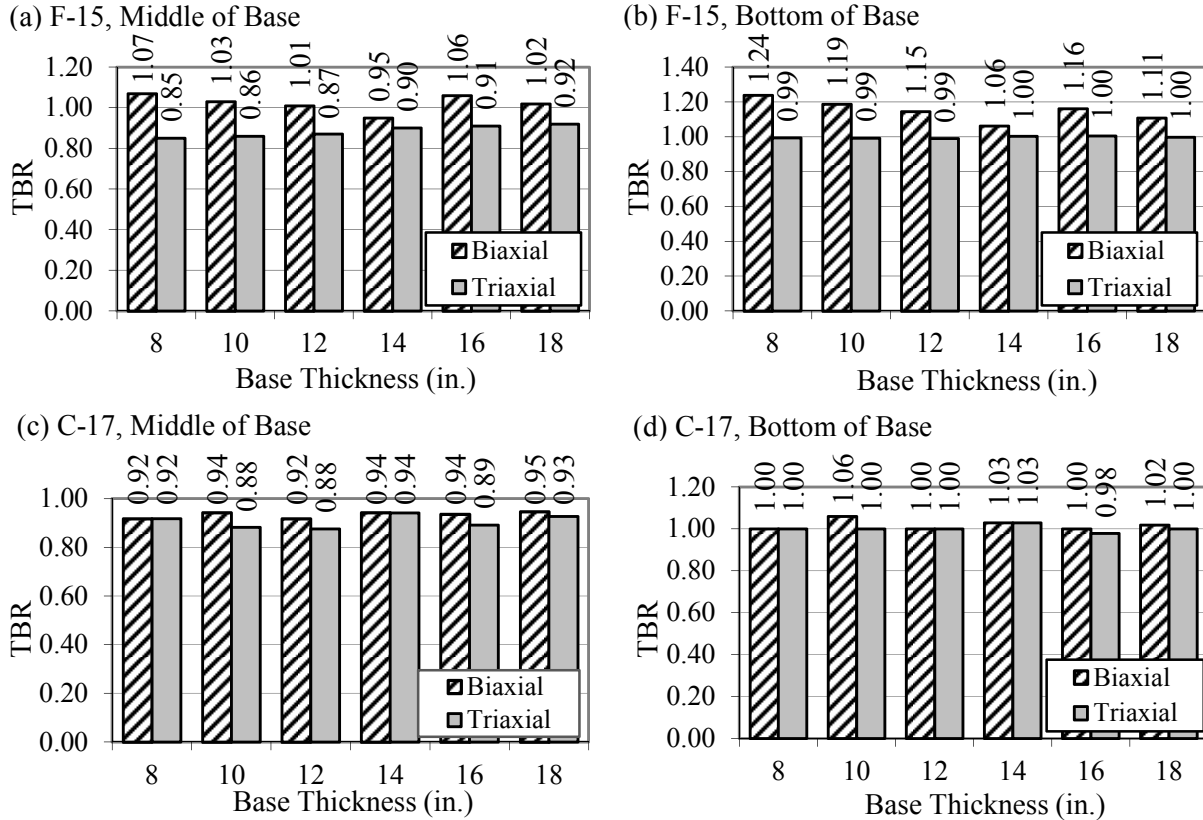


Figure 6. Variation of Traffic Benefit Ratio (TBR) with Respect to Base Thickness for Biaxial and Triaxial Geogrid Reinforced, 3-in. Asphalt Pavement for F-15 and C-17 Aircrafts.

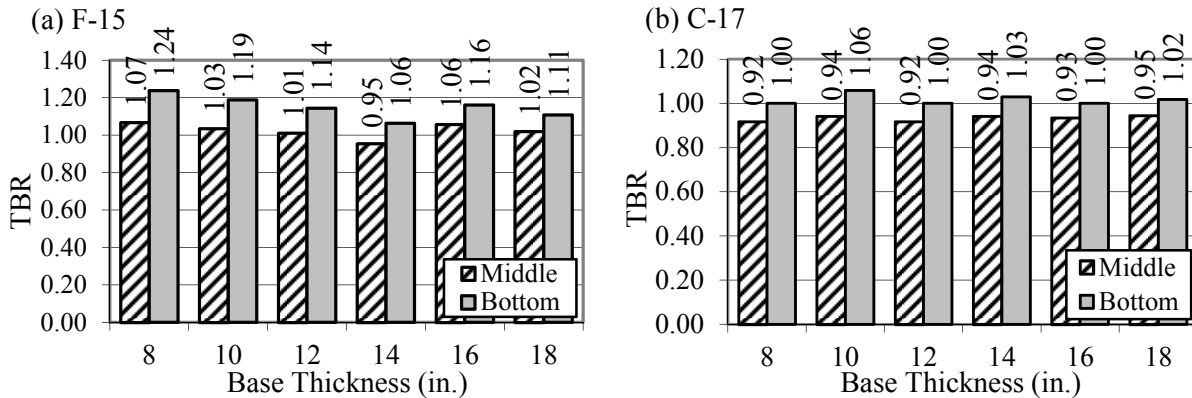


Figure 7. Variations of Traffic Benefit Ratio (TBR) with Respect to Base Thickness in Rutting for a 3-in. Asphalt Pavement for F-15 and C-17 Aircrafts.

to the subgrade and, as a consequence, it is exposed to more rutting than the pavements reinforced at the bottom of the base.

Unlike the F-15 aircraft landing gear, which consists of a single tire with high pressure, the C-17 landing gear consists of 6 tires that distribute the load over a wide area. As such, more rutting is expected in the subgrade rather than in the base. The variations in the number of passes of C-17 with base thickness followed the same trends as the F-15. However, the pavement can

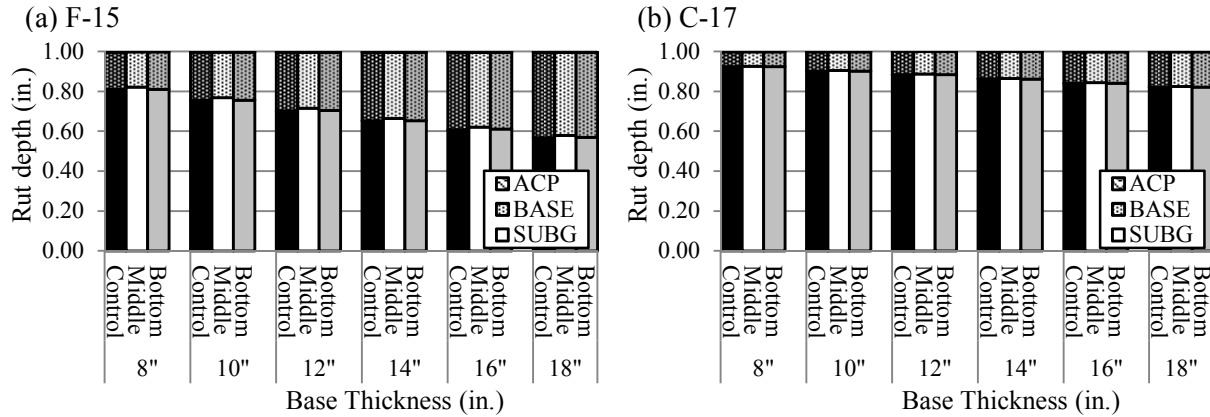


Figure 8. Variation in Rut Depth by Layer at Failure (1 in.) with Respect to Base Thickness for 3-in. Asphalt Pavement for F-15 and C-17 Aircrafts.

endure more passes of F-15 aircrafts than C-17 aircrafts for any base thickness. Figure 7b indicates no clear improvement in the pavement life when geogrid reinforcement is used. The pavement experiences failure earlier than the same pavement unreinforced when the reinforcement is placed in the middle of the base layer. Figure 8b shows the subgrade contributes between 93% and 84% of the total rut, a larger contribution when compared to the subgrade rutting caused by the F-15 aircraft. Rut depths of the HMA layer do not exceed 0.1% of the total rutting while the base layers contribute about 6% to 16% of the total rutting as the base becomes thicker. Despite exerting lower pressure to the pavement surface, higher stresses are generated in both the base and the subgrade layers as compared to the stresses generated by the F-15 aircraft. This is the consequence of the larger contact areas of the tires and the influence of adjacent tires within the axle group. Unlike the F-15, no benefit is observed from the use of the geogrid reinforcement in the base for thin asphalt pavements as most of the rutting stems from the subgrade.

The effectiveness of the geogrid for different HMA thicknesses was evaluated for the two types of landing gears using a base thickness of 10 in. The number of passes to failure in rutting considerably increased as the HMA layer thickness increased. In addition, the HMA contributed more to rutting as it became thicker. For the F-15, the thickness of the HMA does not seem to impact the TBR significantly, shown in Figure 9. However, under the C-17 landing gears, the TBR decreases as the thickness of the HMA increases as long as the geogrid is placed at the bottom of the base.

IMPACT OF BASE AND SUBGRADE MODULUS

As reflected in Figure 10, the effectiveness of the geogrid (as judged by TBR) diminishes as the base layer becomes stiffer. Thus, it is more reasonable to use geogrids with weaker bases. The benefits of the geogrid are more realized when they are placed at the bottom of the base. The traffic benefit ratios for a 3-in. asphalt and 10-in. base geogrid reinforced pavement with different subgrade moduli are shown in Figure 11 for both F-15 and C-17 landing gears. The use of the geogrid reinforcement at the bottom of the base proved to be more beneficial in pavements with weaker subgrades under the F-15 landing gears. On the other hand, the use of geogrid reinforcement in the middle of the base layer was more beneficial for pavements with stiffer

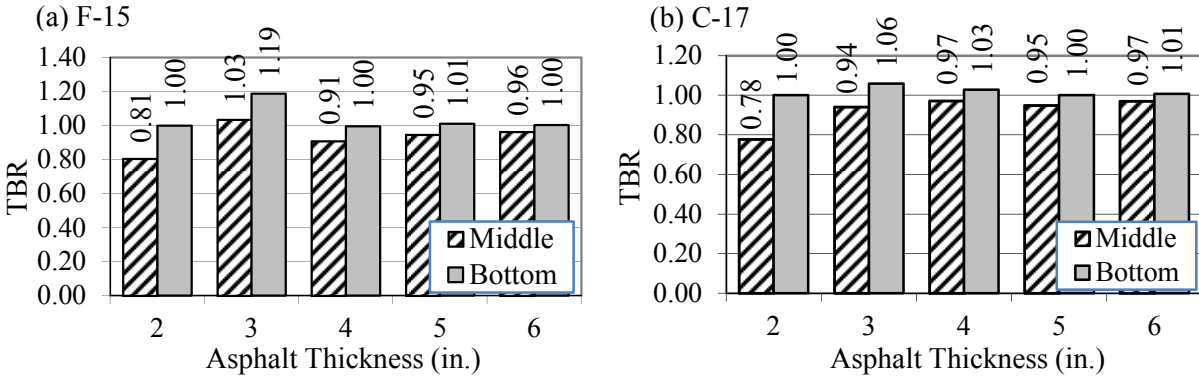


Figure 9. Variation of Traffic Benefit Ratio (TBR) with Respect to Asphalt Thickness in Rutting for a 10-in. Base.

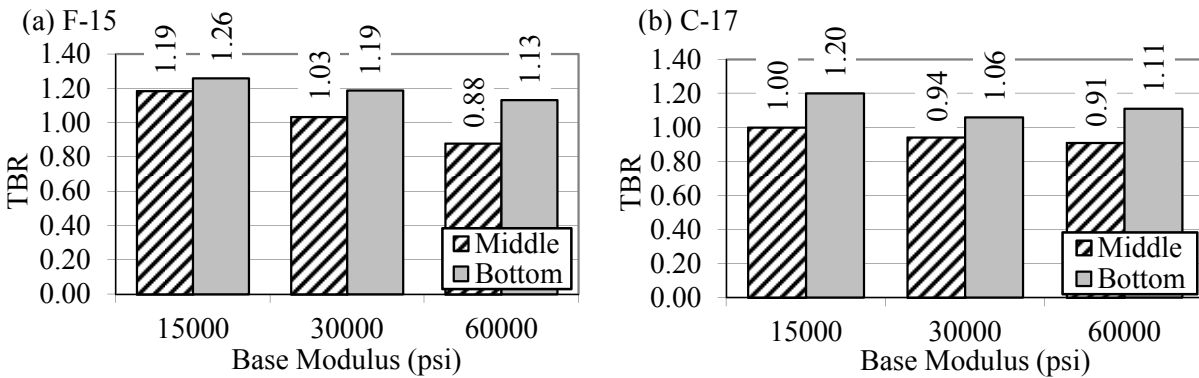


Figure 10. Variation of Traffic Benefit Ratio (TBR) with Respect to Base Modulus in Rutting for a 3-in. Asphalt and 10 in. Base.

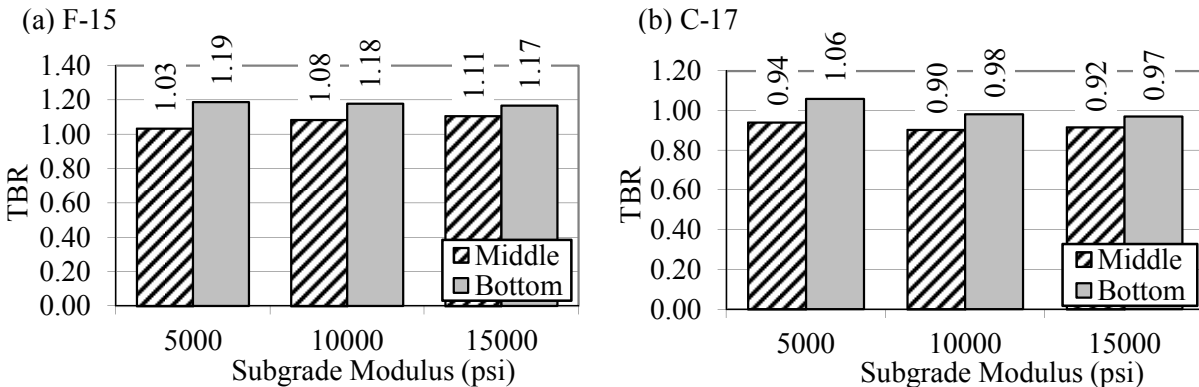


Figure 11. Variation of Traffic Benefit Ratio (TBR) with Respect to Subgrade Modulus in Rutting for a 3-in. Asphalt and 10 in. Base.

subgrades. The contribution of the subgrade to the total rutting diminishes as the subgrade becomes stiffer and, as a result, the base layer gains relevance in its contribution to total rutting. Moreover, the use of geogrid reinforcement at the middle of the base reduces the rutting in the base layer more than when used at the bottom of the base. The TBR values for the C-17 landing gears are always less than unity, except when the subgrade modulus is 5000 psi and the geogrid reinforcement is placed at the bottom of the base layer. As the subgrade modulus increases, the rutting is transferred from the subgrade to the base. About 90% of the total rutting for a 5000 psi

(36 MPa) subgrade is from the subgrade, while about 70% of the total rutting is stemmed from the subgrade for a 15,000 psi (103 MPa) subgrade. Thus, for this type of loading, geogrid reinforcement does not seem to be beneficial.

IMPACT OF GEOSYNTHETIC REINFORCEMENT OF BASE COURSE TO THICKER UNREINFORCED BASES

The benefit of utilizing a thicker base vs. utilizing reinforcement was also evaluated. In this case, TBR is defined as the ratio of number of passes to reach failure for a reinforced base to that of an unreinforced base that is 2 in. thicker. As shown in Figure 12, the addition of 2 in. of base seems to be more beneficial than adding the geogrid, especially for thinner bases.

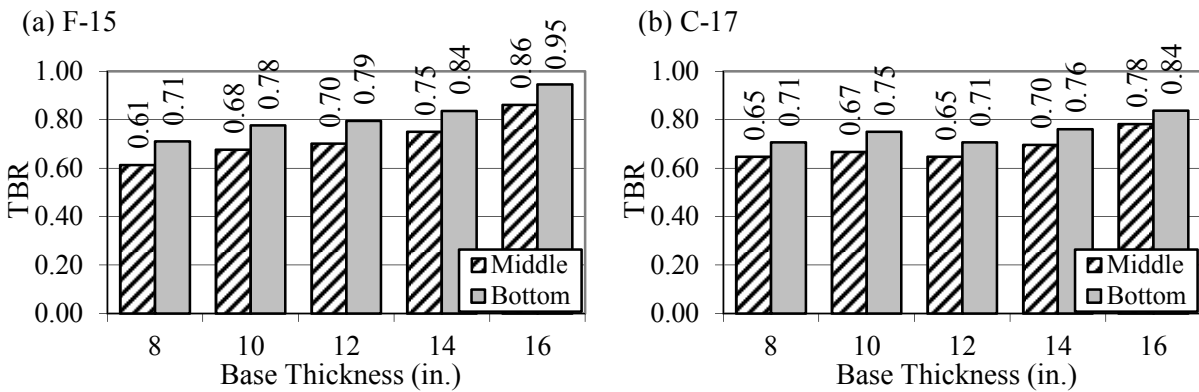


Figure 12. Variation of Traffic Benefit Ratio (TBR) with Respect to Base Thickness in Rutting for a 3 in. Asphalt Pavement with TBR Computed from an Unreinforced Base with Additional 2-in. Thickness.

SUMMARY

Parametric studies were carried out to document the structural benefits that are gained by introducing the geosynthetic materials and possible modifications that can be implemented to typical airfield pavement sections. The most relevant properties, including the type of geosynthetic used (geomembrane or geogrid), soil-geogrid interface shear stiffness, and the type of geogrid (biaxial vs. triaxial), were evaluated. In addition, the impacts of linear vs. nonlinear material models, base thickness and modulus, HMA thickness, and subgrade modulus were considered. The findings from the parametric studies are summarized in Table 6. This table presents the sensitivity of relevant parameters to the TBR values.

The following conclusions can be outlined: The TBR is moderately sensitive to the thickness of the HMA. The TBR is more significant for thin asphalt layers. The TBR values are sensitive to thickness and modulus of the base mainly when the reinforcement is placed at the interface of the base and subgrade layers, and when the F-15 type loading is applied. The sensitivity diminishes for thicker bases and is accentuated for less stiff bases. The effectiveness of geogrid reinforcement is significantly impacted by the modulus of the subgrade. As the subgrade becomes stiffer, the percentage of rutting in the base layer increases. A significant component to the effectiveness of the geogrid is the type of the geogrid used (as quantified by the soil/aggregate-geogrid interface shear stiffness), particularly when the geogrid reinforcement is

placed in the middle of the base. Based on the information that was available, no clear additional benefit was observed for the triaxial geogrid when compared to the biaxial geogrid. This conclusion may change when more concrete information or standard test procedure become available about the interface shear stiffness. Generally, the geogrid is more beneficial when a pavement is trafficked by F-15 rather than C-17 aircrafts. This is attributed to the loading and axle characteristics of C17 that causes larger deformations within the subgrade. It must be mentioned that the values presented hereby were not calibrated with actual field results and as such the results and conclusions are relative in nature.

Table 6.
Details of Aircraft Gears Considered for Parametric Studies.

Property		Aircraft Type			
		F-15		C-17	
		Location of Geogrid			
		Middle	Bottom	Middle	Bottom
Biaxial Geogrid					
HMA	Thickness				
Base	Thickness				
	Modulus				
Subgrade	Modulus				
Soil/Aggregate-Geogrid Interface	Shear Stiffness				
Triaxial Geogrid					
Base	Thickness				
Geotextile/Geomembrane					
Base	Thickness				

 Not significant: $0.95 \leq TBR \leq 1.05$
 Moderately significant: $0.90 \leq TBR < 0.95$ and $1.05 < TBR \leq 1.10$
 Significant: $TBR < 0.90$ and $TBR > 1.10$

REFERENCES

1. Berg, Ryan R., Christopher, Barry R. and Perkins, Steven W., "Geosynthetic Reinforcement of the Aggregate Base Course of Flexible Pavement Structures," GMA White Paper II, Geosynthetic Materials Association, Roseville, MN, p. 130, 2000.
2. Perkins, Steven W., and Edens, Michael Q., "Finite element and distress models for geosynthetic-reinforced pavements," *International Journal of Pavement Engineering*, Vol. 3, No. 4, pp. 239-250, 2002.
3. Uzan, J., "Characterization of granular materials," *Transportation Research Record*, 1022, pp. 52-59, 1985.
4. Federal Highway Administration, "VESYS 5Ws User Manual, Truck Pavement Interaction Program," Office of Infrastructure Research and Development, Federal Highway Administration, U.S. Department of Transportation, 2003.

5. National Cooperative Highway Research Program, "Guide for Mechanistic-Empirical Design of New and Rehabilitated Pavement Structures." Final Report – NCHRP Project 1-37A, Transportation Research Board, National Research Council, Washington, DC, 2004.
6. von Maubeuge, K., and Lesny, C., "Reinforcement of Base Courses with Geogrids - Related Issues," *GeoAmericas 2008*, The First Pan American Geosynthetics Conference and Exhibition, Cancun, Mexico, 2-5 March, pp. 936-943, 2008.
7. Kinney, Thomas C., and Xiaolin, Y., "Geogrid aperture rigidity by in-plane rotation," Geosynthetics Conference, Vol. 2. Nashville, pp. 525–537, 1995.
8. Perkins, S.W., Christopher, B.R., Cuelho, E.L., Eiksundd, G.R., Hoff, I., Schwarts, C.W., Svanø, G., Want, A., "Development of Design Methods for Geosynthetic Reinforced Flexible Pavements," FHWA Report DTFH61-X-00068, Final Report, Federal Highway Administration, Washington, D.C., 2004.
9. Kwon, J., "Development of mechanistic model for geogrid reinforced flexible pavements," Ph. D. thesis, Univ. of Illinois at Urbana-Champaign, Urbana, IL, 2007.
10. Perkins, Steven W., "Numerical modeling of geosynthetic reinforced flexible pavements." FHWA Report No. MT-01-003/99160-2, U.S. Dept. of Transportation, Federal Highway Administration, Washington, D.C., 2001.